POLITECNICO MILANO 1863

SCUOLA DI INGEGNERIA INDUSTRIALE E DELL'INFORMAZIONE

EXECUTIVE SUMMARY OF THE THESIS

Development of a multibody model for the estimation of elastic and damping parameters in running prosthetic feet

TESI MAGISTRALE IN BIOMEDICAL ENGINEERING - INGEGNERIA BIOMEDICA

AUTHOR: Chiara Usai

ADVISOR: Nicola Francesco Lopomo

CO-ADVISOR: Andrea Giovanni Cutti, Roberto Di Marco, Francesca Gariboldi, Marco Palombi

ACADEMIC YEAR: 2025-2026

1. Introduction

Running-specific prostheses (RSPs) are devices designed to enable Paralympic athletes perform high-intensity locomotor activities such as running and jumping; their key component is the running-specific prosthetic foot (RPF), a carbon fiber blade engineered to store elastic energy during the loading phase and return it during push-off, partially replacing the biomechanical function of the biological ankle-foot complex. The mechanical characterization of these devices, in terms of stiffness and energy dissipation, is essential for optimizing prosthetic configuration in Paralympic athletes and for supporting athletic performance and design decisions [1] [2]. However, no standardized protocol currently exists for the objective quantification of RPF mechanical properties.

This thesis was conducted in collaboration with the INAIL Prosthetics Centre of Vigorso di Budrio (Bologna, Italy), a national center of excellence for prosthetics research and Paralympic sports technology, which collaborates directly with elite athletes and tests high-performance devices in competitive settings.

The study focuses on two models of carbon fiber RPFs: the Össur Cheetah Xceed (C-shaped profile, Category 2), used by an athlete with transfemoral (TF) amputation, and the Össur Cheetah Xtreme (J-shaped profile, Categories 4, 5 and 6), used by an athlete with transtibial (TT) amputation. The primary objectives are: (i) to develop a lumped-parameter model and assess its capacity to reproduce the experimental ground reaction force (GRF) curves and the characteristic distance, defined as the distance between the upper and lower extremities of the blade and used as a proxy for its compression, through quantitative comparison based on the normalized root-mean-square error (nRMSE); (ii) to identify, by means of Particle Swarm Optimization (PSO), the equivalent torsional stiffness K* [N·m/deg] and the equivalent damping coefficient D* [N·m·s/deg] for each prosthetic configuration and speed range; (iii) to assess the biomechanical plausibility of the identified parameters as a function of prosthetic category and running speed. This work proposes an original methodology combining multibody simulation and dynamic identification of elastic and dissipative parameters from real sprint data for the biomechanical characterization of sports prosthetic feet.

2. Materials and Methods

2.1 Experimental Data Acquisition

Kinematic and kinetic data were acquired during 60-metre sprint trials at the Palaindoor facility in Padova [3]. The measurement system included:

- 10 Vicon Vantage V5 infrared cameras (stereophotogrammetric system)
- 9 AMTI force platforms (sampling rate ~1000 Hz for kinetics, ~100 Hz for kinematics)

Two Paralympic athletes participated:

- **TF athlete** (male, 65 kg, 180 cm): Össur Xceed Cat 2 on the left side witch Ottobock 3S80 monocentric prosthetic knee. Four pylon-height configurations evaluated (A: 75 cm, B: 95 cm, C: 55 cm, D: 54 cm).
- **TT athlete** (male, 76 kg): Össur Xtreme on the right side. Three stiffness categories evaluated (A: Cat 5, B: Cat 6, C: Cat 4).

Trials were performed at two intensity levels: 50–70% of personal best (PB) and 100% PB. A total of fifty trials across two sessions were collected and processed.

The data processing pipeline used the open-source Olympia software (MATLAB-based), which reconstructed marker trajectories, computed joint angles and segment rotations, and extracted the ground reaction force (GRF) window centered on the GRF peak for each selected step.

2.2 Multibody Model Implementation

Using Matlab/Simulink, the external profile of each RPF was discretized into sixteen rigid segments connected in series. The number of segments was determined by minimizing the geometric error between the CAD profile and the segmented approximation, selecting the minimum number for which the error fell below 1 mm²/mm for both prosthetic feet. The model to be implemented can be expressed as a segmented representation of the prosthetic foot's external profile, in which a torsional spring-damper element (K, D) is introduced at the main curvature, with the system's kinematic inputs (translation (x, y, z) and rotation about the y-axis) derived from the Olympia software

The Simscape Multibody model consists of:

- **16 Solid blocks** (rigid segments) connected by Rigid Transforms encoding inter-segment angles from the segmentation,
- A **Cartesian Joint + Revolute Joint** at the clamp, imposing the measured 3D translation and pitch angle as kinematic inputs,
- A **torsional spring-damper** implemented as a Revolute Joint with elastic (K*) and viscous (D*) components, placed between segments 7 and 8 (optimal position determined by comparing mean optimization error across three candidate locations: 5-6, 6–7, 7–8),
- A **three-ellipse sole** (attached under segments 14–15–16 via Weld Joints) interacting with a rigid Infinite Plane via the **Spatial Contact Force** block (Smooth Spring-Damper normal model; Smooth Stick-Slip friction model).

The total simulated GRF is the sum of the three contact force contributions. The characteristic distance between the clamp origin and the marker of segment sixteen is measured via a Transform Sensor.

2.3 Parameter Identification via PSO

The two unknown parameters K* [N·m/deg] and D* [N·m·s/deg] were identified by minimizing a cost function J via Particle Swarm Optimization (PSO): $J(K,D) = 0.5 \cdot \varepsilon_{\mathrm{GRF}} + 0.5 \cdot \varepsilon_{\mathrm{dst}}$ where each error term ($\varepsilon_{\mathrm{GRF}}, \varepsilon_{\mathrm{dst}}$) is the normalized RMSE (nRMSE) between the simulated and experimental signal, normalized by the signal range:

$$\varepsilon_{\mathrm{norm}} = \frac{\mathrm{RMSE}}{\max(y) - \min(y)}$$

Search bounds for K were derived from experimental estimates of the instantaneous torsional stiffness:

$$K(t) = \frac{M_y(t)}{\Delta\theta(t)} = \frac{b(t) \times \mathrm{GRF}(t)}{\theta(t) - \theta(t_0)}$$

where M_y is the moment of the compression axis and $\Delta\theta$ is the angular deflection from the unloaded posture. The bounds for D* were set to [0.01, 1] N·m·s/deg based on physical considerations (underdamped regime for composite materials).

The PSO used twenty particles and thirty iterations per trial, a compromise between solution accuracy and computational cost (each evaluation requires a full Simulink simulation run).

2.4 Mechanical Quantities Derived

Beyond K* and D*, the following quantities were computed for each trial:

- Compressive deformation:
  $$\Delta d = d_0 - d(t)\ [\mathrm{m}]$$
  where d_0 is the pre-loading distance between clamp and tip,
- Equivalent compressive stiffness:
  $$K_c = \frac{\mathrm{GRF}(t)}{\Delta \mathrm{d}(t)} \left[\frac{kN}{m}\right]$$
- Angular deformation:
  $$\Delta\theta = \theta_0 - \theta(t)\ [\mathrm{deg}]$$
  used for GRF–$\Delta\theta$ hysteresis analysis.

Model accuracy was quantified using the normalized RMSE (nRMSE), expressed as a percentage and normalized with respect to the range of reference signal, computed both on individual trials and on group mean curve.

3.6 Statistical Analysis

Non-parametric tests (Mann-Whitney U, Kruskal-Wallis + Dunn-Bonferroni post-hoc) were applied to K* and D* across groups and velocity bands (α = 0.05).

3. Results

3.1 GRF vs. Time

The simulated GRF curves (Figure 1) reproduce the global shape of the experimental reference across all configurations. A systematic initial spike is present in all simulated curves immediately after touch-down (values between 1500 and 3000 N), absent in the experimental data.

Table 1. nRMSE for GRF by group.

Group	nRMSE [%] individual trials	nRMSE [%] mean curves
TF	10.27 ± 2.28	6.56
TT	17.22 ± 3.90	14.08
TT-A (Cat 5)	16.48 ± 2.16	13.97
TT-B (Cat 6)	16.41 ± 6.19	13.81
TT-C (Cat 4)	19.38 ± 3.41	17.30

The TF configuration achieves the best agreement (nRMSE = 6.56% on mean curves). The TT group shows higher errors.

3.2 Characteristic Distance vs. Time

The simulated distance curves (Figure 2) reproduce the compression–decompression pattern in all categories, with a plateau phase, progressive decrease to a minimum at mid-stance, and a slower return compared to the experimental data.

Table 2. nRMSE for characteristic distance by group

Group	nRMSE [%] individual trials	nRMSE [%] mean curves
TF (Cat 2)	10.06 ± 2.93	7.89
TT	8.90 ± 2.31	7.81
TT-A (Cat 5)	9.00 ± 2.34	8.54
TT-B (Cat 6)	9.90 ± 2.92	7.90
TT-C (Cat 4)	7.70 ± 0.95	7.46

The distance metric shows consistently lower errors than GRF.

3.3 Optimized Parameters K* and D*

PSO converged for all fifty trials. Key findings:

Equivalent torsional stiffness K* (Figure 3**):**

- Range: 13 to 22 N·m/deg across all configurations,
- Increases with prosthetic category,
- Decreases with running speed (higher K* at sub-maximal velocities).

Equivalent damping D:*

- Range: 0.15 to 0.50 N·m·s/deg,
- TT groups show systematically higher values than TF,
- Increases with prosthetic category.

3.4 GRF vs. Angular Deformation

As $\Delta\theta$ decreases (negative values corresponding to progressive blade compression), GRF increases, reaching peak values of approximately 1500–2500 N for TF and 2000–2800 N for TT at maximum angular deflections of -20° to -25°. Loading and unloading branches are systematically separated in all configurations, forming a hysteresis loop. The separation is more pronounced in TT groups and near toe-off ($\Delta\theta \rightarrow 0°$).

3.5 Equivalent Compressive Stiffness Kc

The Kc curves show a non-linear profile in all configurations: stiffness rises progressively during the loading phase, reaching a peak at maximum compression, and decreases during unloading. Peak experimental Kc values:

- **TF (Cat 2):** 18–19 kN/m at 40–60 mm deformation
- **TT-C (Cat 4):** ~25 kN/m
- **TT-A (Cat 5):** ~24–25 kN/m at ~90–100 mm
- **TT-B (Cat 6):** up to 32 kN/m

3.6 Statistical Analysis

Torsional stiffness K:*

- TF vs. TT: $\mathbf{p < 0.001}$ (large effect, $|r| > 0.5$),
- Post-hoc: TF significantly different from all TT categories (TF vs. TT-C and TF vs. TT-B: $p < 0.01$; TF vs. TT-A: $p < 0.001$),
- Comparisons between TT categories: not significant,
- Velocity effect: significant in TT group ($p < 0.001$); significant only for TT-A (Cat 5) at category level ($p < 0.05$).

Equivalent damping D:*

- TF vs. TT: $\mathbf{p < 0.001}$,
- Post-hoc: TF vs. TT-C ($p < 0.01$), TF vs. TT-A ($p < 0.001$), TF vs. TT-B ($p < 0.01$); TT-A vs. TT-B ($p < 0.05$),
- Velocity effect: significant only for TT-A (Cat 5) ($p < 0.05$).

4. Discussion

The results obtained from the multibody model demonstrate an overall satisfactory agreement with experimental data across both prosthetic profiles and amputation levels, while also providing a set of mechanical parameters that characterize the elastic and dissipative behavior of the running-specific prostheses under real dynamic loading conditions.

The model reproduces the overall GRF profiles with nRMSE ranging from 6.56% to 14.08% on mean curves. Among all configurations, the TF group achieves the best agreement, while TT-C shows the highest error. The reduction of errors on mean curves compared to individual trials indicates that part of the trial-to-trial variability is physiological due to running strategy, step-to-platform alignment, instantaneous velocity, rather than a structural model limitation. The main residual discrepancies between simulated and acquire data are a systematic initial GRF spike immediately after touch-down (reaching 1500–3000 N, in some trials exceeding the central peak by over 500 N), a slightly premature toe-off (approximately 10–20 ms earlier than measured). These artifacts are attributable to: the punctual contact model at touch-down, which assumes instantaneous point interaction rather than the distributed pressure generated by the finite sole geometry; the rigid ground assumption, whereas real athletics track surfaces exhibit non-negligible viscoelastic behavior depending on material, thickness and aging state [4], the simplified sole geometry modeled as three consecutive ellipses; and the pitch-only kinematic input, which neglects out-of-sagittal-plane rotations. It is worth noting that the experimental GRF reflects not only the intrinsic RPF properties but also the interaction between blade geometry, sole mechanical characteristics and ground surface factors only partially captured by the present model [2].

The nRMSE values for the characteristic distance (7.46–10.06% on individual trials, 7.46–8.54% on mean curves) are consistently lower than those for GRF across all groups, confirming that the model captures kinematic deformation more accurately than contact dynamics. This is expected: the characteristic distance depends primarily on model geometry and imposed clamp kinematics, whereas GRF is additionally sensitive to contact stiffness, friction coefficients and pressure distribution. The slightly better performance observed for the TT group on this metric is partly attributable to the virtual nature of the J-profile clamp, which eliminates the geometric measurement errors that affect the physical C-profile clamp reconstruction in Simscape. The slower simulated decompression observed in the final part of the stance is consistent with the linear nature of the spring model, which cannot reproduce the non-linear unloading behavior of the composite blade.

The optimized K* values are biomechanically plausible: they increase progressively with prosthetic category defined by the manufacturer (higher categories corresponding to greater stiffness) consistent with the nominal stiffness hierarchy. Unlike the categorical classification provided by producers, which assigns discrete stiffness levels without objective mechanical values, the proposed model returns a quantitative and directly comparable estimate of torsional stiffness for each tested configuration, enabling discrimination within and across categories. K* decreases at higher running speeds consistently with published findings where the fixed blade stiffness dominates the prosthetic limb response and prevents the active modulation that biological limbs achieve through muscle co-activation at proximal joints [5] . This behavior contrasts with the near-constant leg stiffness of non-amputee runners across speeds. The equivalent damping D* shows systematically higher values in TT categories than TF, and a general increase with prosthetic category, suggesting that greater structural stiffness is associated with greater energy dissipation during the loading cycle. The simultaneous identification of K* and D* via PSO does not allow to exclude partial numerical compensation between the two parameters.

The GRF–Δθ plots reveal systematic hysteresis in all configurations: the unloading branch lies below the loading branch for the same angular deformation, indicating that part of the elastic energy stored during compression is dissipated during the stance cycle. This separation is more pronounced in TT groups consistent with the greater deformation amplitudes and peak forces reached by higher-stiffness categories. This behavior is physically attributable to the viscoelastic nature of carbon fiber composite, well established in the RSP literature[1]. It directly justifies the inclusion of D* in the model: in a purely conservative system the two branches would coincide, whereas the observed separation is qualitatively consistent with the damping values identified via PSO.

The equivalent compressive stiffness Kc values are consistent in range with published bench-test data for comparable RPF blades, including the Ottobock 1E90 Sprinter characterized by Doyen et al. [4] at 0° configuration. The non-linear profile of Kc, with stiffness rising progressively during loading and decreasing during unloading. This non-linearity is not captured by the present model, which adopts a single torsional spring with constant stiffness throughout the entire stance phase: a simplification that is functional to the optimization procedure but limits the ability to reproduce local stiffness variations associated with the progressive redistribution of load along the blade geometry. Introducing a non-linear spring characteristic represents therefore a natural and prioritized direction for future model development.

5. Conclusions

This work assessed the methodological feasibility of a lumped-parameter multibody model for the dynamic characterization of RPF from real sprint data. The model demonstrated acceptable predictive accuracy for both GRF and characteristic distance, with PSO-identified parameters showing biomechanically plausible trends across prosthetic categories and velocity levels. Current limitations include the reduced sample size, the linear spring assumption, the simplified contact model, the pitch-only kinematic input, and the lack of comparable literature for direct numerical validation of K* and D*. These points define the roadmap for future developments, which should focus on non-linear modeling, refined contact mechanics, larger cohorts and energetic analysis linking the identified parameters to sprint performance. The simultaneous dynamic identification of equivalent torsional stiffness K* and damping coefficient D* from real sprint data represents the primary novelty of this contribution, going beyond existing quasi-static bench characterization approaches and opening a new methodological direction for the dynamic characterization of running prosthetic feet.

Bibliography

[1] O. N. Beck, P. Taboga, and A. M. Grabowski, "Characterizing the Mechanical Properties of Running-Specific Prostheses," *PLoS One*, vol. 11, no. 12, p. e0168298, Dec. 2016, doi: 10.1371/journal.pone.0168298.

[2] L. Rahnama, K. Soulis, and M. D. Geil, "A review of evidence on mechanical properties of running specific prostheses and their relationship with running performance," *Frontiers in Rehabilitation Sciences*, vol. 5, Jun. 2024, doi: 10.3389/fresc.2024.1402114.

[3] R. Di Marco *et al.*, "A motion capture protocol for the kinematic analysis of transfemoral and transtibial sprinters," *Front. Bioeng. Biotechnol.*, vol. 13, Nov. 2025, doi: 10.3389/fbioe.2025.1655295.

[4] É. Doyen, F. Szmytka, and J.-F. Semblat, "A novel characterisation protocol of mechanical interactions between the ground and a tibial prosthesis for long jump," *Sci. Rep.*, vol. 13, no. 1, p. 5226, Mar. 2023, doi: 10.1038/s41598-023-31981-2.

[5] C. P. McGowan, A. M. Grabowski, W. J. McDermott, H. M. Herr, and R. Kram, "Leg stiffness of sprinters using running-specific prostheses," *J. R. Soc. Interface*, vol. 9, no. 73, pp. 1975–1982, Aug. 2012, doi: 10.1098/rsif.2011.0877.

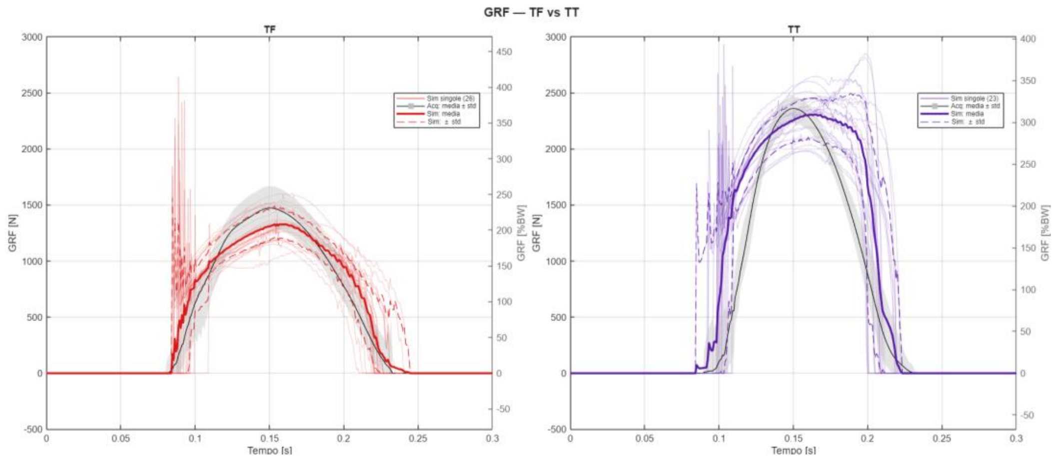

Figure 1. GRF as a function of time for the two prosthesis groups.

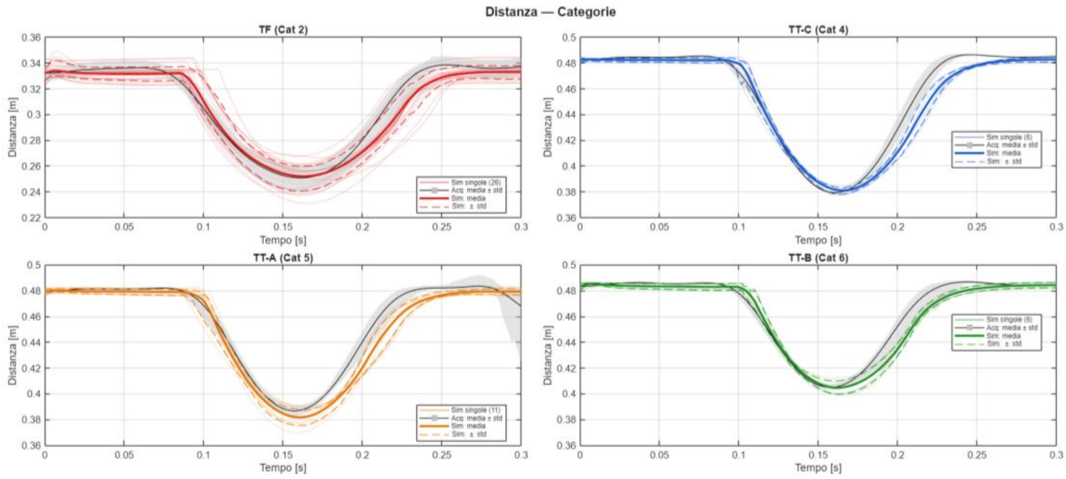

Figure 2. Characteristic distance as a function of time for the four categories.

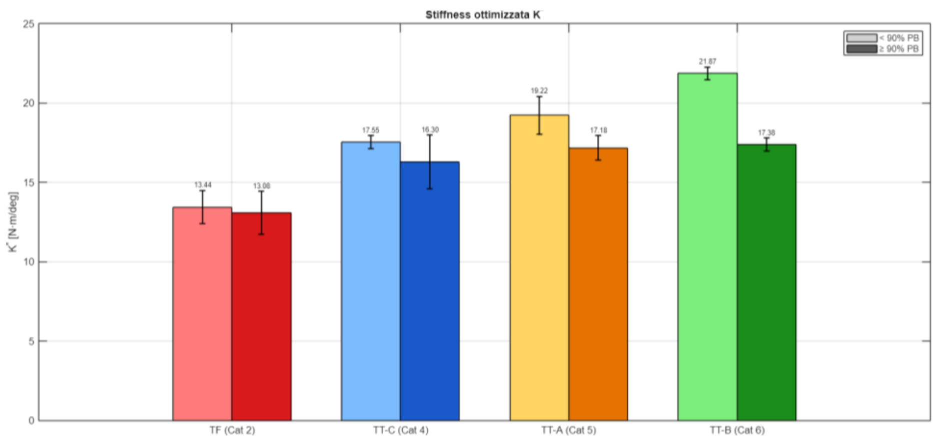

Figure 3. Histograms showing the mean torsional stiffness parameter K*, divided according to running speeds greater than or equal and lower to 90% PB.